Crystallinity of Polyamide 6 Staple Fibers in the Felt Structure Under Simulated Paper Machine Conditions

Tomi Hakala,[1] Ali Harlin[2]

[1]*Fibre Materials, Department of Materials Science, Tampere University of Technology, FIN-33101, Tampere, Finland*
[2]*VTT Technical Research Centre of Finland, P.O. Box 1000, FIN-02044 VTT, Espoo, Finland*

Received 23 March 2010; accepted 12 September 2010
DOI 10.1002/app.33424
Published online 10 December 2010 in Wiley Online Library (wileyonlinelibrary.com).

ABSTRACT: Polyamide 6 (PA6) is used in staple fibers and yarns in paper machine press felts due to its good mechanical properties. The crystalline modifications (α and γ forms) and the degree of crystallinity of PA6 can change under stress (compression) and heat (friction), which are present during mechanical dewatering (nip). Here, we investigate the effects of the molecular weight and crystallinity of a polymer on the mechanical properties of PA6 staple fibers such as wear resistance and compaction. The experimental part involves the ageing of felt specimens in a wet pressing simulator. The properties of the felt (air permeability), and the durability and branching of the staple fiber are examined as functions of the wear of a press felt and the crystallinity of the polymer. The changes that take place in the PA6 polymer are investigated using several techniques, and their connection with the properties of a new or aged press felt is discussed. The results indicate that the increase in molecular weight has a beneficial effect on the material's mechanical properties, and our observations also support previous studies on the crystallinity and branching of PA6. © 2010 Wiley Periodicals, Inc. J Appl Polym Sci 120: 2222–2232, 2011

Key words: ageing; crystal structures; molecular weight; polyamides; staple fibers

INTRODUCTION

Special textiles in the paper making process are known as paper machine clothing (PMC) materials. The materials and structure of these textiles are selected according to the required properties of the end product (paper or board) and the paper machine (PM) applications and processing conditions. They are thus tailor made for specific locations and individual positions in the PM. One of these textiles is a press felt, which transfers, guides, and supports a wet paper sheet in the wet pressing section. This resilient and permeable felt provides a uniform pressure distribution in the nip (the gap between two rolls) providing for efficient dewatering and runnability. Felts consist of carded and preneedled batt layers with staple fibers and woven base fabric(s) with yarns. These synthetic materials are spun from polyamide (PA) polymers.[1,2] Wear resistance and resilience are important for press felts in the harsh processing conditions. At the end of its life, the effect of wear can be seen as severely deformed staple fibers, both on the paper side (PS) and the roll side (RS) of the felt. A decrease in thickness indicates the effect of compaction. Naturally, the staple fibers and yarns require high tensile strength as fiber breaks have a severe impact on paper quality causing problems in paper converting and printing machines.

Stresses impacting on the press felts arise from the felt preparation and paper making processes. The materials in press felts are under mechanical stress during their preparation (carding and needling); so fiber degradation, and even breaks in the fiber, can be initiated here. Under PM conditions, the fiber can be degraded both mechanically and chemically. Mechanical degradation can be initiated by both external and internal abrasions in the press section such as a high compressing force in the nip, friction in the nip-and-press-felt interface, and structural friction in the press felt. In addition, press felts are subject to the effects of different paper chemicals, (additives and fillers) and high pressure showers used during maintenance work (mechanical and chemical washing).[3] The particles of the filler can get jammed between fibers and yarns in the felt during the papermaking process. Such jamming speeds up as the felt becomes more compacted. Depending on the filler types, they can glue fibers to each other or to contaminants inside the felt. Furthermore, hard filler particles can rub the surface of the fibers causing wear, resulting in fibrillation or fiber breaks. The compacted and contaminated press felt is removed from the process after 30–90 days due to its reduced

Correspondence to: T. Hakala (tomi.hakala@tut.fi).
Contract grant sponsor: Rhodia's Groupe API.

dewatering properties and/or runnability.[1–3] Maximum felt life can be prolonged by regular inspection and maintenance, thus reducing the PMC costs, unscheduled PM shutdowns, and/or rejection and complaints from the customer.

Extensive research has been done on PMs' runnability, nip dewatering, and process simulation. The information from these studies and R and D work on press felt materials and structures have improved the durability and felt life. For example, runnability problems and insufficient dewatering are caused by batt layers, if the resilience and durability of the staple fibers are poor. The resilience and ageing of press felts has been studied[4] using a rapid nip strike method, Hopkinson Split Bar (HSB), where wet pressing was simulated under both dry and wet conditions. The HSB results confirm the link between the resilience loss and the wear of the press felts. On the basis of the studies of Strnad et al.,[5] the structure and surface morphology of the polyamide 6 (PA6) fibers can be modified by high temperature, under a vacuum or in specific solutions, resulting in changes to the fibers' reactivity. The study of changes in reactivity of PA6 fiber is interesting and it partly explains the increased contamination of a press felt during its life. The mechanical degradation of the fiber has been studied under laboratory conditions using conventional textile test methods such as the yarn abrasion tester (Zweigle G 552). For example, in a study by Cayer-Barrioz et al.,[6,7] fibrillation was attained in a similar test device, in which static staple fibers were rubbed under water by a rotating rod. However, their rubbing method was inadequate for PMC materials, since this test only causes damage to certain parts of the staple fibers and does not take the presence of linear load (nip) and paper chemicals (filler) into account. Consequently, the test does not effectively replicate the conditions and dynamic stresses to which press felt and its raw materials are subjected during wet pressing. These aspects need to be included in studies of press felts. Accelerated ageing test methods, such as laboratory-scale wet pressing simulators, have been developed because trials on PMs are very time consuming, costly, and difficult to schedule into the production program.[8,9] For example, our single-nip construction with a filler spraying system simulates harsh wet pressing conditions in the PM. The principles of our wet pressing simulator and ageing methods are described in another article.[10]

Polyamide

Different types of synthetic PA (PA6, PA66, and PA6.10) are semicrystalline, consisting of both amorphous and crystallized areas. They are also hydrophilic in that the water absorption capacity increases when the number of carbon atoms is decreased and *vice versa*. Their degree of crystallinity and the crystal structures themselves are affected by processes such as spinning, drawing, and heating. Process parameters, such as speed, draw ratio, and annealing, have an impact on the orientation of macromolecules. Generally, a high degree of crystallinity gives better mechanical properties for synthetic fibers, but excessive crystallinity of PA6 can lead to brittle fracture, lower impact strength, stress cracking, and failure of the polymers. Furthermore, the crystallization process of PA6 can continue after the preparation process; e.g., while in storage on the bobbin, due to its low glass transition temperature (T_g).[11–14]

The fiber PA6 (ε-caprolactam) has many valuable properties for press felts such as good abrasion resistance, elasticity, and an ability to return to its original dimensions after stress. Resilient PA6 fibers are important in press felt so that it can resist compaction and filling in. The wear rate of PA6 is 10^{-15} m^3/Nm, and it is resistant to most chemicals. The melting temperature (T_m) is quite high (210–220°C), and its T_g is quite low (40–85°C). The low T_g of PA6 is beneficial for surface calendaring resulting in a smooth felt; the smoother the felt's surface, the lower the risk of felt marking on the paper sheet. The coefficients of static and kinetic friction for pure PA6 are 0.22 and 0.26, respectively.[15,16] Sufficient friction between the rolls and felts is necessary for the PM to run. However, polyamides do have disadvantages such as low thermal stability and susceptibility to sunlight and pilling.[17]

The crystallinity of polymers can be analyzed using several methods such as X-ray diffraction (XRD), differential scanning calorimetry (DSC), Fourier transform infrared (FTIR), and solid-state nuclear magnetic resonance (NMR).[12,17–19] Polymer PA6 has α- and γ-crystalline forms, both of which have a monoclinic cell unit with different lattice parameters (Fig. 1). Furthermore, metastable forms of PA6 (β and δ) have also been observed. The α form is more stable than the γ form because its degree of ordering of crystallinity is higher. The γ form can be converted to the α form by chemicals, heating, and/or stress (pressure or stretching) and this transformation can be reversed by treatment with iodine. In analytical studies, including mechanical tests, it has been observed that while the α form has higher tensile strength, the γ form has greater ductility.[5,13,20–24] The studies of Konishi and Ito,[25] Litvinov and Penning,[26] and Vasanthan[14] have reported the crystalline densities for amorphous, α and γ forms; the range of density values being 1.08–1.09 g/cm^3, 1.23–1.24 g/cm^3, and 1.16–1.19 g/cm^3, respectively. In the work of Devaux et al.,[27] it was reported that the melting points for the α and γ forms are about 220°C and 212°C, respectively. The variations in densities

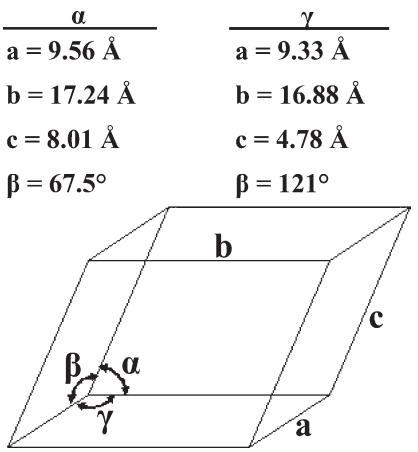

Figure 1 Values of unit cell parameters relating to α and γ forms of PA6.

and melting points of the crystalline and amorphous forms partly explain why the density (1.13–1.14 g/cm^3), T_g and T_m of PA6 varies in literature.[15,18,28]

The properties of PA6 can be modified under several production and polymeric processes to more accurately meet the requirements of specific applications. For example, PMC material suppliers have developed high-molecular-weight PA polymers of staple fibers with chemical additives in the batt layers to improve resistance to friction, wear, contamination, and chemical degradation.[3,8,9,29,30] Another technique is to use polymer branching as, given the same molecular weights, the melt viscosity of PA6 is lower in a branched polymer than in a linear one. The lower melt viscosity allows the processing of higher molecular weight polymers at lower temperatures and pressures.[31–34] The link between a lower T_m and polymer branching of PA6 is reported in the work of Risch et al.[32] They found differences in crystallization half times and reduced reptation times between linear, 3-arm and 6-arm PA6 polymers. On the basis of the analytical studies of Dai et al.,[34] the number of star-shaped molecules and the length of branched chains have an impact on the mechanical properties of PA6. They found that star-shaped PA6 polymers had lower strength, elongation, and initial modulus than linear-chain polymers. However, the star-shaped polymer chains had better elasticity and recovery from stress. The branching of PA6 polymer thus seems to have potential for improving the lifetime of press felt materials; an increase in molecular weight leads to better elasticity and resilience for felt materials and structures. Based on a literature search, few research publications have dealt with the polymer structure and wear properties of PA6 staple fibers.

In our study, the felt specimens were prepared using PA6 staple fibers and yarns supplied by Rhodia Technical Fibers. After the felt specimen preparation, it was aged under simulated wet-pressing conditions. The properties of five staple fiber types with different molecular weights were measured using several different analyzers to determine the crystalline forms and the degree of crystallinity. Finally, we studied the felt's properties and staple fiber's durability as a function of the wear of the press felt and the polymer crystallinity and molecular weight. The structural properties of press felts and other polyamide qualities were outlined in our study.

EXPERIMENTAL

Materials

Staple fiber specimens

At the beginning of the study, the molecular weights (M_w) of five staple fiber types were measured. We determined the molecular weights (a viscosity average molar mass) with the dilute-solution viscosity method, using the single-plate spindle of a Brookfield viscometer. Formic acid was the solvent, and several concentration fractions of each PA6 specimen were prepared; the weight fractions of the PA6 being 2.5%, 5%, 7.5%, and 10% in the polymer solution. We also had two reference PA6 polymers with known molecular weights for comparison. The polymer solution was heated for 30 min at 40°C and mixed with a rotating magnet tap. After overnight cooling, the viscosities were measured. Then, the molecular weights were determined using graphical plots of the reduced viscosity and concentration of the polymer solutions, and graphical plots of their intrinsic viscosity, and molecular weight. The following Mark-Houwink-Sakurada equation[20] was used for the calculations:

$$[\eta] = KM^{\alpha} \quad (1)$$

where [η] is the intrinsic viscosity, M is the molecular weight, K is the Mark-Houwink-Sakurada coefficient (slope), and α is the Mark-Houwink-Sakurada coefficient (exponent). Based on our calculations, the coefficient values were 0.509 for α and 0.017 for K. The fiber specimens (SF-1, SF-2, SF-3, SF-4, and SF-5) with their molecular weights (M_w) are shown in Table I. The staple fiber specimens had clear variations in molecular weights; SF-1 was a medium-molecular-weight polymer; SF-2, SF-3, and SF-4 were high-molecular-weight polymers; and SF-5 was an ultrahigh-molecular-weight polymer.

Press felt specimens

We used staple fiber types for the felt preparation except for SF-3; so, the measured values (crystallinity) of SF-3 only apply to the raw staple fiber.

TABLE I
Staple Fiber Specimens and the Mean Values of Their Molecular Weight (M_w)

	Staple fiber specimen	Molecular weight (g/mol)
1	SF-1	81,036
2	SF-2	105,752
3	SF-3	131,971
4	SF-4	132,460
5	SF-5	154,326

The felt specimens were prepared from a woven, single-layer base fabric, which had been attached to carded and preneedled batt layers by the needling. Two batt layers (2×300 g/m^2) were on the PS and one batt layer (400 g/m^2) was on the RS. The staple fiber fineness was 22 dtex in all the batt layers. The fabrics were made from the same monofilament yarns for the warp and weft. Their diameter was 0.3 mm and the fineness was 810 dtex. The staple fibers tangled with each other during the mechanical needling and created many contact points between themselves and the staple fibers and yarns. After needling, the specimens were heat treated on the PS at 170°C. After preparation, each felt specimen was 1500 mm long and 240 mm wide. The thickness of the felt specimens varied between 4.5 and 5.0 mm. The felt specimens were made into an endless loop by sewing their ends together—the seams being excluded from the analyses. As our purpose was to study the properties and modifications of the staple fiber types, we decided to keep the structure of the felt as simple as possible and the preparation conditions as gentle as possible. Naturally, preparation processes and conditions were the same for all felt specimens. Nevertheless, some minor damage (scratches) to the staple fibers and yarns during the preparation process was unavoidable.

Before the ageing tests the air permeability, thickness and mass per unit area of the porous felt specimens were measured in the laboratory. These measurements ensured the quality of the specimens and a specimen was rejected if unusual variations in properties were found either in the machine direction (MD) or the cross machine direction (CMD).

Accelerated ageing test

In the ageing test, we used a 2-mm wide nip, calcium carbonate ($CaCO_3$) as filler, and a washing system for felt cleaning. Table II shows the settings for our ageing tests including nip pressure, speed, number of cycles, etc. Nip pressure was high because of short nip length and high linear load (8.34 kN/m). The running speed (90 m/min) was much lower than in papermaking (1300–2000 m/min); the higher speed being unsuitable because of felt wrinkling. The temperature (30°C) was lower than in the actual papermaking process (60–70°C). The higher temperature was excluded because its control could not be guaranteed.

The ageing test for each of the press felt specimens involved 300,000 nip strikes and lasted for 3 weeks. A total of 100,000 cycles were reached after 5 working days. At the end of each day, the felt specimen was cleaned with a washing system requiring about 2000 cycles. The washing removed the remains of the filler solution from the specimen and enabled the felt to be reused the next day. After every "ageing week," the moist felt specimens were dried in a laboratory room under standard temperature and atmospheric conditions (EN 20139: 1992); the relative humidity was 65 ± 2% and the temperature was 20 ± 2°C. After 24 h of drying, the air permeability, thickness, and mass per unit area of the aged felt specimens were measured in the laboratory after 100,000; 200,000; and 300,000 cycles. After the measurements, small strips were cut from the edge of the aged felt specimen for visual examination and to identify any structural modifications or extended wear, using the Philips XL-30 scanning electron microscope (SEM). SEM pictures were taken of single staple fibers, surfaces and cross sections of new (nonaged) and aged felts.

Characterization of staple fibers

In addition to the SEM inspections, the staple fiber specimens were taken from raw staple fiber bundles, and new and aged press felt specimens for analytical measurements. The analytical measurements were carried out in the research laboratories: test parameters and conditions were chosen based on the researchers' experience and know how.

X-ray diffraction

Wide-angle X-ray scattering (WAXS) measurements were made at the University of Helsinki in the X-ray Physics Division of the Department of Physical Sciences. Their measurement apparatus consisted of a Rigaku X-ray generator equipped with a rotating

TABLE II
Test Parameters Used in the Ageing Tests

Parameter	Value
Pressure	255 kp (4.17 Mpa)
Speed	90 m/min (1.5 m/s)
Temperature	30°C
Ageing cycles/week	100,000
Washing cycles/day	2000
Duration	3 weeks (15 days)

copper anode, a silicon crystal monochromator, and a Mar345 image plate scanner. The operating parameters were 50 kV and 60 mA. The Kα copper line corresponded to a wavelength of $\lambda = 1.5418$ Å. The distance from the vacuumed X-ray tube to the specimen was $\sim$ 2.7 m, and the distance between the specimen and the imaging plate was $\sim$ 0.2 m. The beam size was adjustable through horizontal and vertical slits. The air scattering was eliminated by taking a background measurement without a specimen and this background measurement was subtracted from the diffraction patterns. Moreover, amorphous background was determined by measuring the melted PA6 fiber specimen. Measurements were carried out in ambient temperature and pressure. Before the WAXS measurements, the fibers were extracted from raw fiber bundles and felt surfaces. Then, they were cut into pieces, ground into powder, and dried in the exsiccator for 40 h. After the measurements, the crystallinity was calculated by determining the difference between the total intensity and the scattering intensity from the amorphous phase and dividing this by the total intensity.

The measurements of grazing incidence X-ray diffraction (GIXRD) were taken with the X'Pert PRO MRD® instrument in the Application Laboratory XRD of PANalytica Co. The XRD instrument consisted of a parabolic mirror, a parallel plate collimator (0.27°), a ceramic Cu long fine focus tube, and software for the measurements and analyses. The operating parameters were 45 kV and 40 mA. The diffractometer radius was 0.24 m, and the beam size was 1.2 mm by 24 mm in the equatorial and axial planes, respectively. The measurement geometry was chosen so that the beam only penetrated the top of the specimens. For the XRD measurements, the specimens were tested in the following ways: the raw staple fibers were measured using a piece from a fiber bundle, whereas the staple fibers of new and aged press felts were measured directly on the surfaces of the felt pieces (PS and RS). Therefore, before being measured, the felt pieces (600 mm^2) were cut and glued to the microscope slide on their PS or RS. After taking the measurements, the profile fitting of data was done using the Pearson VII function of ProFit 1.0® software. All intensities of curves were normalized on the first intensity peak α(200) to ease comparison. The diffracted intensities of the peaks, α(200), γ(020), α(020), and amorphous form, were calculated from the peak area divided by the sum of the diffracted intensity areas, including the amorphous peak.

DSC and FTIR

The DSC measurements were carried out using the Netsch DSC 204 F1 instrument at Tampere University of Technology (TUT) in the Plastics and Elastomer Technology Laboratory of the Department of Materials Science. Two specimen preparations were used as follows: cut, short fiber pieces, and wound fiber bundles. In both cases, the fiber specimens ($\sim$ 10 mg) were dried for 36 h at 60°C before the DSC measurements were taken. The measurements were done in a nitrogen environment and the heating rate of 10°C/min from 25 to 280°C was selected. The heating was performed twice for the fiber specimens.

Fourier transform infrared (FTIR) measurements were made at TUT in the Chemistry Laboratory of the Department of Chemistry and Bioengineering. The FTIR instrument type was the Perkin–Elmer Spectrum One FTIR Spectrometer equipped with a Perkin–Elmer Universal ATR Sampling Accessory. The penetration depth of the diamond ATR crystal was 1.66 μm, and the spectral range was 4000 cm^{-1}–650 cm^{-1}. Before FTIR measurement at TUT, each fiber specimen was melted for 1 min at 240°C and pressed into a thin film. After these measurements, the IR spectrums of the fiber specimens were analyzed.

RESULTS AND DISCUSSION

Ageing tests and sources of fiber degradation

The evaluation of the properties of the press felts during ageing tests was based on SEM pictures and included a comparison of the measured values of each property (air permeability, thickness, and mass per unit area) as well as visual comparison. The SEM pictures in Figure 2 gives a good example of the compaction of the press felt and the deformations of the staple fibers on the aged felt surface after 300,000 cycles; the compaction and reduction in thickness are obvious in the cross-sectional pictures [Fig. 2(A,B)] indicating changes in air permeability measurements. The degradation of the staple fibers [Fig. 2(C,D)] is also obvious on the felt surface. The shape of the fibers has changed from circular to flat, the edges of the flat staple fibers are torn, the fibers are stretched axially, and some of them are broken. Furthermore, visual checks reveal that the staple fibers have been orientated in the direction of rotation on both sides of the press felt. Fiber deformation and breaking were observed in every staple fiber specimen at the end of the ageing test. These imperfections in the staple fibers also increased the clogging of the press felt; flat fibers decreased the surface porosity and hindered felt cleaning.

The trend in the changes was observed using the mean values of the properties at different ageing stages. The staple fiber deformed and the press felt compacted rapidly during the first 100,000 cycles.

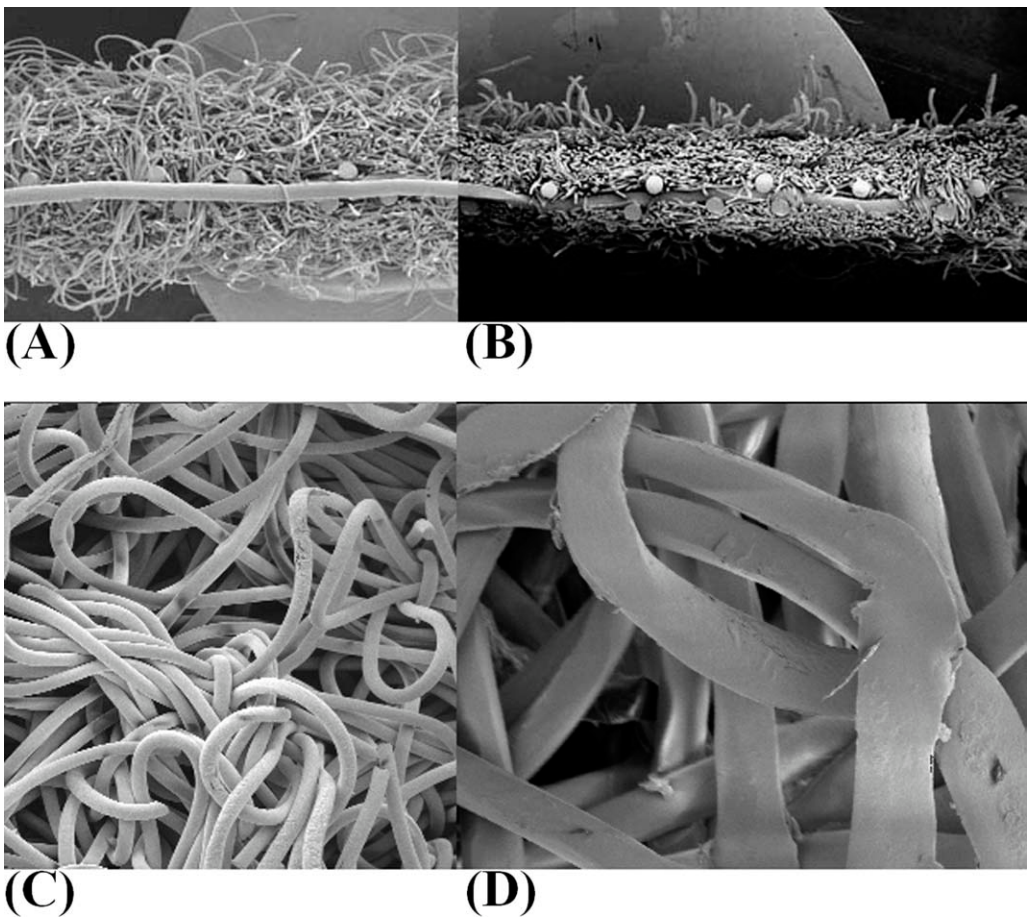

Figure 2 Cross-sectional SEM pictures (×10) from new (A) and aged felt specimens (B) with noticeable compaction. SEM pictures (×25 and ×100) of the staple fiber specimens before (C) and after 300,000 cycles (D) on the paper side of the felt.

The rate of change then became steady, and between 200,000 and 300,000 cycles, the values only dropped slightly. The air permeability, thickness, and mass per unit area of the press felt specimens before and after the ageing tests (300,000 cycles) are compared with the molecular weights of the staple fibers in Figure 3, where the values of the specimens are shown vertically—and the same applies to Figures 4, 6, and 7. The relative reduction varied between −57.6% and −61.6% in air permeability, −6.6% and +2% in mass per unit area, and −45.7% and −63.6% in thickness. Thus, the reduction was greatest for air permeability and thickness. The alteration in mass per unit area was modest—except with SF-4, whose mass per unit area was slightly increased. The change in properties does not show a linear relationship to the molecular weight of the staple fiber specimens; e.g., in air-permeability, SF-2 has the highest value before ageing and its relative reduction is higher than for other specimens. On the other hand, it seems that new and aged press felts with high- or ultra-high-molecular-weight polymers (SF-2, SF-4, and SF-5) were in general more open and bulky than the felt with a medium-molecular-weight polymer (SF-1).

The order of felt specimens was evaluated after ageing. The specimens SF-1 and SF-2 seemed to be less resistant to wear; e.g., SF-2 was the only felt specimen, whose base fabric could be seen through the batt layer after the ageing test. The reason for this was the reduction in felt thickness and the resilience of the staple fibers. After an overall evaluation of the SEM pictures, observations of wear resistance and property reduction in press felts revealed that the best staple fiber was SF-5, the worst was SF-1 or SF-2, and SF-4 was between these extremes. The order of superiority was hard to determine, since changes in properties were not linear or consistent and they depended on whether the specimen was new or aged as well as the ageing stage which had been reached. On the basis of the ageing tests, we concluded that an increase in molecular weight increases wear resistance.

During ageing, felt and staple fiber specimens were simultaneously influenced by two mechanical wearing factors; external and internal abrasion. The

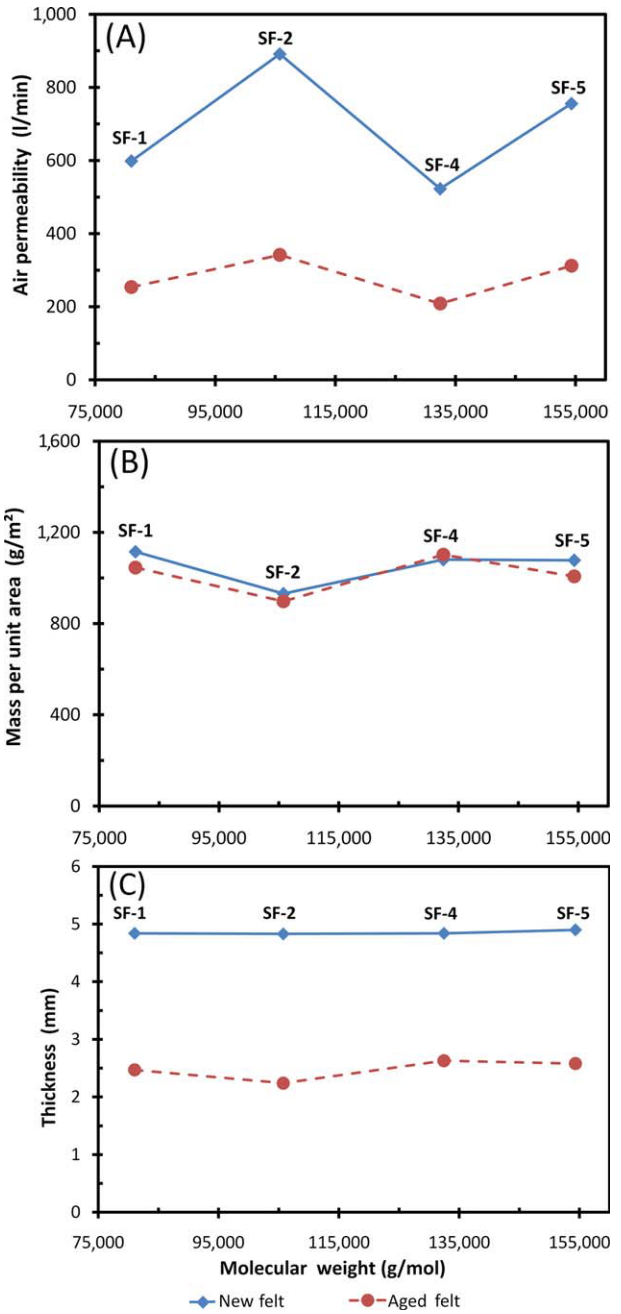

Figure 3 Molecular weights of raw staple fibers, SF-1, SF-2, SF-4, and SF-5, compared with the air permeability (A), mass per unit area (B), and thickness (C) of new (◆) and aged felt (●) specimens (300,000 cycles). [Color figure can be viewed in the online issue, which is available at wileyonlinelibrary.com.]

external abrasion of the specimens was induced by the nip pressure and ceramic bars of the suction box. Furthermore, the moving rolls of our wet pressing simulator generated shear stress through their curvature, the friction forces on the felt specimen in contact areas, and the deformations in the staple fibers. The internal abrasion was caused by the friction between the fibers and the filler solution spray. The hard $CaCO_3$ particles of the filler solution were jammed inside the felt specimen, or to be more precise, between the deformed fiber materials, causing abrasion and clogging. External forces, such as pressure and tensile stress, generated dynamic movements in the fibers. At first, the interfiber friction resists continuous dynamic stress but then the wearing of the fibrous materials reduces fiber bonding and the whole felt structure begins to loosen. On the other hand, the rate of this loosening is countered by the compaction of the felt specimen.

Crystallinity

Analytical measurements from the PA6 polymers of new and aged felts reveal how much the crystallinity changes during ageing. Furthermore, the impact of felt preparation and heat treatment on crystallinity are observed, when comparing the results of raw staple fibers and the fibers from new felts, and also when the fibers from the PS and RS are compared. The total effect on wear can be estimated when the results from laboratory tests during ageing and the analytical measurements are compared.

Table III and Figure 4 show the crystallinity values of the fiber specimens from the WAXS measurements (Division of X-ray Physics). There were no great variations between the specimens and usually there was a drop in the degree of crystallinity after the press felt was made, although specimen SF-4 is an exception. Furthermore, ageing did not significantly change the degree of crystallinity in the staple fibers; usually, the level of change, increase or decrease, was higher on the RS of the felt specimens. The impact of ageing on the degree of crystallinity was lower than the impact of the press felt manufacturing, which was counter to our expectations. On the basis of this unexpected observation, we assume

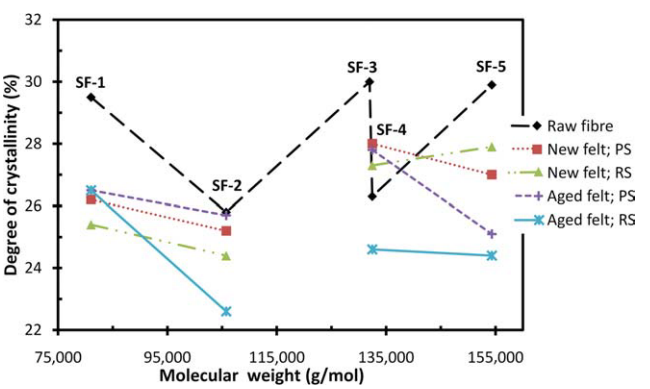

Figure 4 Molecular weights of raw staple fibers, SF-1, SF-2, SF-3, SF-4, and SF-5, compared with the degree of crystallinity; raw staple fiber (◆), staple fiber of new felt on the paper (■) and roll side (▲); staple fiber of aged felt on the paper (+) and roll side (×). [Color figure can be viewed in the online issue, which is available at wileyonlinelibrary.com.]

TABLE III
Relative Degree of Crystallinity (%) of Staple Fibers

	Staple fiber specimen	Raw fiber (%)	New press felt (%)		Aged press felt (%)	
			PS	RS	PS	RS
1	SF-1	29.5	26.2	25.4	26.5	26.5
2	SF-2	25.8	25.2	24.4	25.7	22.6
3	SF-3	30.0	–	–	–	–
4	SF-4	26.3	28.0	27.3	27.8	24.6
5	SF-5	29.9	27.0	27.9	25.1	24.4

Fiber specimens are taken from raw fiber, and both sides of new or aged press felt; paper (PS) and roll side (RS).

that the friction and heat during the mechanical preneedling and needling processes affect the polymer structure of PA6 staple fibers when staple fibers and needles are in contact. More accurate analysis requires further research. Furthermore, a comparison of the PS and RS for each new felt specimen indicated that the heat treatment on the PS in the felt preparation had a minor influence on the degree of crystallinity, and the crystallinity values of the fibers were usually slightly higher on the PS than on the RS. We also concluded that the influence of heat treatment on the crystallinity of the polymer fades rapidly during ageing due to the harsh conditions. In Figure 4, the increase of molecular weight does not show a linear relationship with the increase in crystallinity. We concluded that it is not possible to detect a correlation between crystallinity changes and molecular weights from the values for raw fibers, or for new or aged press felt staple fibers.

The changes in the degree of crystallinity during ageing indicate modifications in the crystal structures. Figures 5–7 present the diffraction curves and the percentages of diffracted intensities of the X-ray measurements (PANalytica Co). Figure 5 shows the X-ray diffraction curves of the raw staple fibers, where the curves are normalized on the first intensity peak (α(200)) of SF-2. As can be seen, the height of the second intensity peak (α(020)) varies between the staple fiber specimens, but the shapes of the curves are quite similar, there being no extra peaks. The percentages of the amorphous phase, α(200), α(020), and γ(020) reflections of raw staple fibers and staple fibers from new and aged felt specimens are compared with their molecular weights in Figures 6 and 7. In addition, the degree of crystallinity and the values from the PS and RS are shown in Figures 6 and 7, respectively.

Our conclusions from Figures 6 and 7 are as follows:

- The γ(020) reflection presented only a fraction of total crystallinity (2.0–8.3%) in the raw staple fibers and the staple fibers from new and aged felts.
- The divergence between the values of the crystalline and amorphous forms is smaller in the raw fibers than it is for those fibers from new and aged felts. This indicates that the tested PA6 fiber specimens react differently to wear.
- The amorphous phase increased and the total crystallinity decreases when raw fiber is compared with staple fibers from new or aged felts—although there is some divergence with SF-4.
- A comparison of the staple fibers from new and aged felts revealed that the crystallinity values decreased overall in the α(200) and γ(020) reflections due to ageing. However, the changes in γ(020) reflection were very small, and the γ(020) reflection values of the SF-4 increased or decreased according to which side of the felt was observed.

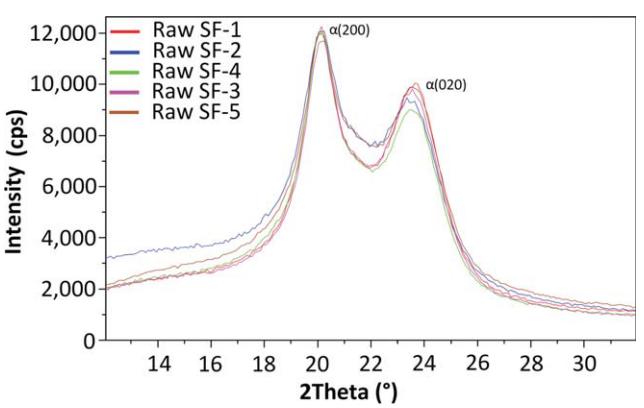

Figure 5 X-ray diffraction curves of the raw staple fibers; the curves are normalized to the first intensity peak of SF-2. [Color figure can be viewed in the online issue, which is available at wileyonlinelibrary.com.]

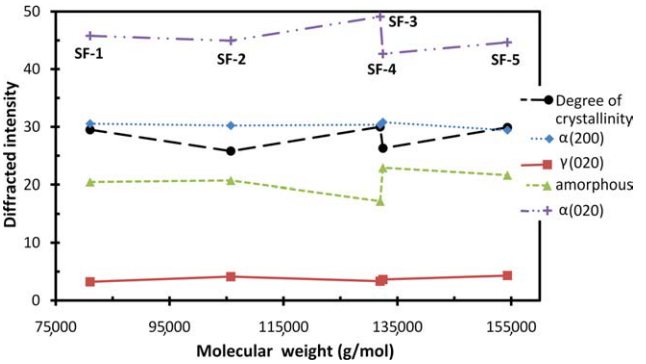

Figure 6 Molecular weights of raw staple fibers, SF-1, SF-2, SF-3, SF-4, and SF-5, compared with the degree of crystallinity (●) and percentage of total diffracted intensities; amorphous (▲), α(200) (◆), γ(020) (■), and α(020) (+) reflections. [Color figure can be viewed in the online issue, which is available at wileyonlinelibrary.com.]

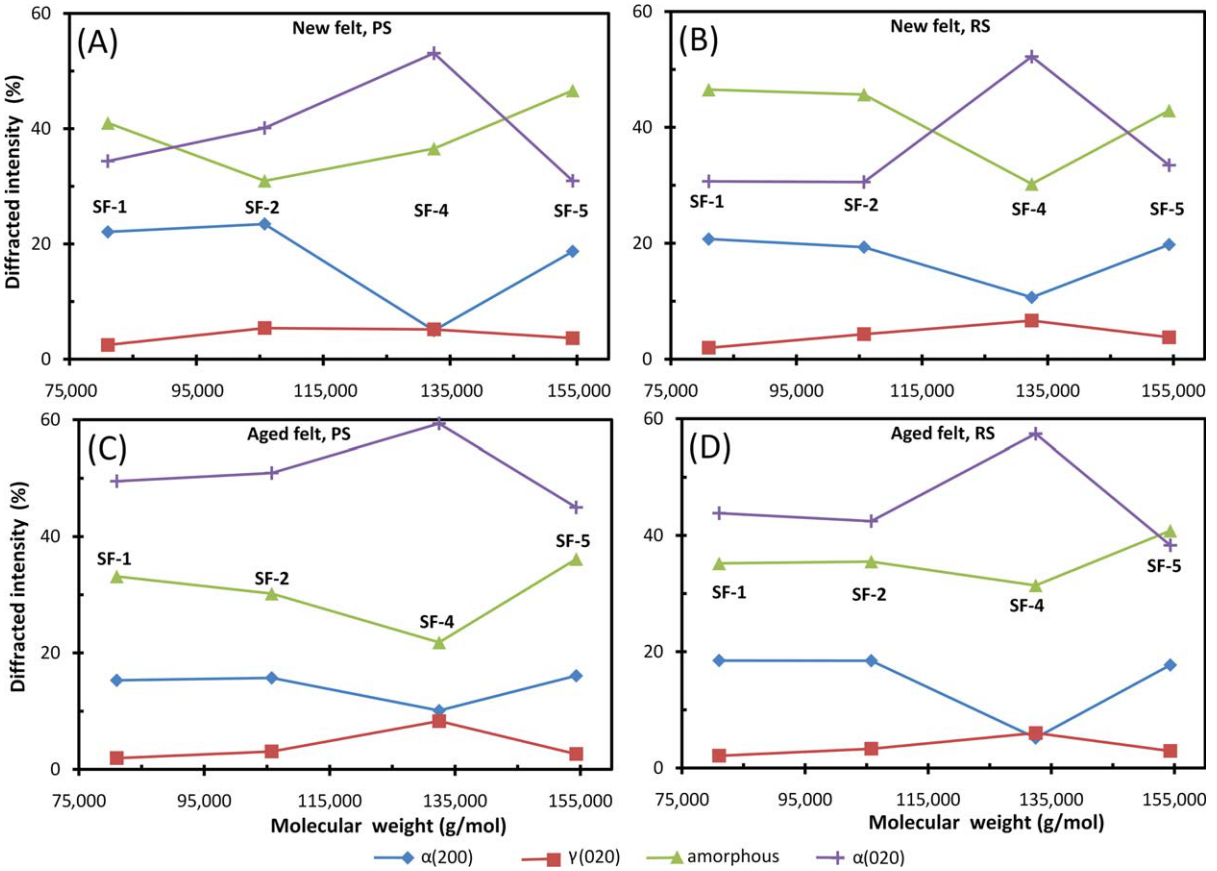

Figure 7 Molecular weights of raw staple fibers, SF-1, SF-2, SF-4, and SF-5, compared with the percentage of total diffracted intensities; amorphous (▲), α(200) (◆), γ(020) (■), and α(020) (+) reflections; staple fiber of new felt on the paper (A) and roll side (B), staple fiber of aged felt on the paper (C) and roll side (D). [Color figure can be viewed in the online issue, which is available at wileyonlinelibrary.com.]

- The values of α(020) reflection increased and those of the amorphous phase decreased during ageing in all specimens—again, there were some minor differences in the case of SF-4.

In summary, the crystallinity of the staple fibers varied widely, and transitions between the amorphous and crystalline phases were observed. We assumed that the transitions between these modifications are caused by stress (compression) and heat (friction) in the nip.

Polymer structure

Comparison of the molecular weights and crystallinity of the raw fibers revealed that the fibers form two groups (Fig. 4): SF-2 and SF-4 in one group and SF-1, SF-3, and SF-5 in the other. The differences between the groups indicated that specimens SF-2 and SF-4 were modified and the assumption is that the latter two specimens were long chain branched (LCB).

Because of the suspicion of modification, the raw staple fibers were measured by FTIR and DSC at TUT. After these measurements, no chemical difference in the fiber specimens was observed on the FTIR curves. The DSC measurements revealed that the melting temperatures of the raw fiber specimens were 224.3°C, 221.6°C, 223.6°C, 222.0°C, and 223.7°C for SF-1, SF-2, SF-3, SF-4, and SF-5, respectively. Thus, SF-2 and SF-4 had a lower T_m. On the basis of these results, we conclude that SF-2 and SF-4 are LCB polymers, with SF-4 having a higher molecular weight.

Finally, we conclude that an LCB fiber with a high molecular weight is in some cases worse than a linear fiber with a low molecular weight. This means that branching without a higher molecular weight has no beneficial effect on the felt's durability. The result can be explained by the difference in their degree of crystallinity. Second, we observed that the felt specimens, which were prepared from LCB staple fibers, had greater bulk and were more open than other felt specimens. Furthermore, we conclude that SF-4 has better wear resistance than SF-2 due to its higher molecular weight (and crystallinity).

Factors affecting the results

Incomplete information from a staple fiber supplier created difficulties for some measurements, and the felt preparation and different analytical methods also had an effect on our analytical results.

In the laboratory measurements, the test points were certain small areas representative of the whole felt specimen, so parallel measurements in CMD and MD were required. Despite the care in felt preparation, the properties varied slightly in CMD and MD, illustrating the nonhomogenous structure of press felt. Naturally, some fiber loss resulted from the specimen cuts. The wear of single staple fibers was variable at the polymer level due to variations in contact area and batt densities (cloudiness). Furthermore, the contaminants in the felt specimens from the ageing tests may have influenced the results and our wet pressing simulator generated high dynamic stress peaks on both the felt and fiber specimens due to its short nip length.

The wear resistance of staple fibers was hard to assess due to the small variations between the staple fibers and the degree of crystallinity of a single fiber changing uncontrollably during ageing. The differences within the XRD measurements, and those between the DSC and XRD measurements can be explained by the differences between the techniques and the preparation of the specimens. These methods use different assumptions for analysis, and separation between the crystalline and amorphous phases can be made on the basis of different characteristics. Furthermore, in the DSC measurements, it was hard to eliminate the presence of water in PA6, even though the staple fibers were dried for a very long time.

The following factors were excluded from our study but need to be included in further research: industrially aged press felts, the analysis of process water contaminant from PM, the tenacity and resilience of a single staple fiber before and after ageing tests, and yarns with branched polymers.

CONCLUSIONS

The significance of the molecular weight and crystallinity of PA6 polymer for the wear resistance of the five staple fibers was investigated. We prepared press felt specimens and aged them in the wet pressing simulator. We used a constant press felt structure and standard test procedures for each staple fiber type.

Our results show that there was a considerable difference between the new and aged materials. The properties of the felt specimens, e.g., air permeability, decreased significantly; the uppermost staple fibers of the felt specimens deformed substantially under linear load and the degree of crystallinity of a single fiber changed during ageing. Contrary to our initial assumption, the degree of crystallinity decreased when raw fibers and fibers from new press felts were compared; the preparation of the press felt specimens having an unexpectedly large influence on the degree of crystallinity. In our opinion, the explanatory factors are friction and heat during the mechanical preneedling and needling processes. On the whole, the degree of crystallinity decreased when fibers from new and aged press felts were compared—but in some cases it increased. The heat treatment on the PS had a minor influence on the degree of crystallinity. After ageing, slight differences were observed between fiber specimens taken from the PS and the RS. The changes in the crystallinity also indicated modifications in the crystal structures. The transitions from amorphous phase to α form and from γ form to α form were observed when the felt was aged. We assume that the transition to α form is caused by stress (compression) and heat (friction) in the nip.

We found that an increase in the molecular weight of PA6 polymer improves the durability of the staple fiber but the degree of crystallinity and the polymer branching also affect the durability of staple fibers. It appears that the molecular weight of PA6 polymers has a greater influence on wear resistance than its degree of crystallinity, and that an increase in crystallinity does not always give a clear indication of the advantages or disadvantages to the properties of the press felt. In addition, branched staple fibers did not improve the wear resistance of the press felt. Indeed, it seemed that a branched PA6 polymer with a low molecular weight has a negative effect on wear resistance.

Naturally, our results do not give an all-embracing answer to specific felt wear problems, but a high-molecular-weight staple fiber (with high crystallinity) without branching seems to be preferable for the felt structure tested in our study. Another conclusion is that changes in press felt design, in the operating conditions, or in other parameters of the papermaking process have a greater effect on the wear of press felts than any individual staple fiber inside the press felt. Nevertheless, in the long run, deformations at the inter- and intrafiber level combine to create structural changes in the press felt.

The authors also thank Prof. Ritva Serimaa, Markus Ovaska, and Mika Torkkeli from the Division of X-ray Physics, Martin Tremblay and Jouko Nieminen from PANalytical Co., and Markus Kakkonen from the Laboratory of Plastics and Elastomer Technology for their analytical measurements. Kind compliments also to the personnel of the Laboratory of Fibre Materials Science—especially to Arja Puolakka for the advice on FTIR.

References

1. Adanur, S. Paper Machine Clothing; Technomic: Lancaster, PA, 1997.
2. Paulapuro, H. Papermaking Part 1. Stock Preparation and Wet End. Book 8; Fapet: Helsinki, 2000.
3. McGuffey, M.; Diamond, E.; Leonard, J. Recognition and Prevention of Press Felt Fiber Loss—Some Practical Considerations; Weavexx Corporation: http://www.xerium.com (accessed 2010).
4. Hakala, T.; Harlin, A.Autex Res J 2008, 8, 84.
5. Strnad, S.; Stana-Kleinschek, K.; Tusek, L.; Ribitsch, V.; Werner, C.; Kreze, T. Macromol Mater Eng 2002, 287, 296.
6. Cayer-Barrioz, J.; Mazuyer, D.; Kapsa, P.; Chateauminois, A.; Robert, G. Polymer 2004, 45, 2729.
7. Cayer-Barrioz, J.; Mazuyer, D.; Kapsa, P.; Chateauminois, A.; Bouquerel, F. Wear 2003, 255, 751.
8. Bottiglieri, J. TAPPI-Solutions for People, Processes and Paper; 2004; Vol. 87, p 70.
9. Bottiglieri, J. TAPPI-Solutions for People, Processes and Paper; 2005; Vol. 88, p 27.
10. Hakala, T.; Wilenius, T.; Harlin, A. Autex Res J 2007, 7, 71.
11. Albrecht, W.; Fuchs, H.; Kittelmann, W.; Nonwoven Fabrics. Raw Materials, Manufacture, Applications, Characteristics, Testing Processes; Wiley-VCH: Weinheim, 2003.
12. Gutmann, R.; Snezana, B. Chem Fibres Int 2005, 55, 107.
13. Dencheva, N.; Denchev, Z.; Oliveira, M. J.; Funari, S. S. J Appl Polym Sci 2006, 103, 2242.
14. Vasanthan, N. J Polym Sci Part B: Polym Phys 2003, 41, 2870.
15. Cook, J. G. Handbook of Textile Fibers. Volume 2: Man-Made Fibres, 5th ed.; Merrow: Durham, 1984.
16. Booser, E. R. Tribology Data Handbook: An Excellent Friction, Lubrication, and Wear Resource; CRC: Boca Raton, FL, 1997.
17. Gruszka, I.; Lewandowski, S.; Benko, E.; Perzyna, M. Fibers Text Eastern Eur 2005, 13, 133.
18. Yang, H. H. In Handbook of Fiber Chemistry, 3rd ed.; Lewin, M., Ed.; CRC: Boca Raton, FL, 2006; Chapter 2.
19. Billmeyer, F. W., Jr. Textbook of Polymer Science, 3rd ed.; Wiley: New York, 1984.
20. Dersch, R.; Liu, T.; Schaper, A. K.; Greiner, A.; Wendorff, J. H. J Polym Sci Part A: Polym Chem 2003, 41, 545.
21. Barret, C. S.; Cohen, J. B.; Faber, J., Jr.; Jenkins, R.; Leyden, D. E.; Russ, J. C.; Predecki, P. K. Advances in X-ray Analysis; Plenum Press: New York, 1986; Vol. 29.
22. Dasgupta, S.; Hammond, W. B.; Goddard, W. A., III. J Am Chem Soc 1996, 118, 12291.
23. Schreiber, R.; Veeman, W. S.; Gabrielse, W.; Arnauts, J. Macromolecules 1999, 32, 4647.
24. Li, Y.; Goddard, W. A. Macromolecules 2002, 35, 8440.
25. Konishi, R.; Ito, M. Polymer 2004, 45, 5191.
26. Litvinov, V.; Penning, J. Macromol Chem Phys 2004, 205, 1721.
27. Devaux, E.; Bourbigot, S.; El Achari, A. J Appl Polym Sci 2002, 86, 2416.
28. Zaremba, S.; Steffens, M.; Wulfhorst, B.; Hirt, P.; Koch, P.-A. Chem Fibers Int 1997, 47, 442.
29. Elkins, P. R. Pulp Pap 2003, 104, 11.
30. Meadows, D. G.; Shearin, R. H. TAPPI J 1995, 78, 44.
31. Coltelli, M.-B.; Angiuli, M.; Passaglia, E.; Castelvetro, V.; Ciardelli, F. Macromolecules 2006, 39, 2153.
32. Risch, B. G.; Wilkes, G. L.; Warakomski, J. M. Polymer 1993, 34, 2330.
33. Gao, C.; Yan, D. Prog Polym Sci 2004, 29, 183.
34. Dai, L.; Huang, N.; Tang, Z.; Hungenberg, K. J Appl Polym Sci 2001, 82, 3184.